Eur. Phys. J. B **39**, 453–457 (2004)
DOI: 10.1140/epjb/e2004-00217-7

THE EUROPEAN PHYSICAL JOURNAL B

The influence of deposition parameters on production of soft $Fe_{81}Co_{13.5}Si_{3.5}C_2$ and $Fe_{67}Co_{18}Si_1B_{14}$ films

H. Kockar[a]

Balikesir University, Science & Literature Faculty, Physics Department, Balikesir, 10100, Turkey

Received 12 December 2003 / Received in final form 1st June 2004
Published online 23 July 2004 –

Abstract. Production parameters are important for the production of desirable type of magnetic materials. The feasibility of low coercivity amorphous films production using a novel rotating cryostat (RC) technique for sensor application was investigated. $Fe_{81}Co_{13.5}Si_{3.5}C_2$ and $Fe_{67}Co_{18}Si_1B_{14}$ amorphous films was vaporised using a resistively heated furnace on to a liquid nitrogen cooled polyimide Kapton^{TM} substrate rotated at the speed of 1300 rpm. The Orthogonal design process was applied in order to systematically optimise the deposition process and parameters over the output functions for the production of low coercivity films. The results indicate that the process can be easily optimised at these level settings with the goal of having the low coercivity amorhous films. By comparing the output function differences with standard deviation for coercivity, the effects of all input parameters (furnace shape, furnace power, mass of material and the gap between substrate and source) on coercivity values of films were analysed. Furthermore, the amorphous nature of these films was confirmed by X-ray measurement.

PACS. 81.10.Bk Growth from vapor – 75.50.Bb Fe and its alloys

1 Introduction

A Novel Rotating Cryostat (RC) system can deposit materials onto surface of a substrate mounted on a rapidly rotating (up to 2000 rpm) liquid nitrogen cooled cylindrical drum under $\sim 10^{-6}$ mbar vacuum. The system has a large deposition area of 80 cm^2 (40 cm in length and 2 cm wide) and up to ten target sources can be placed around the RC. The details of the RC system can be found elsewhere [1–4].

Amorphous materials are most commonly produced in the form of ribbons, wires and have generally a number of superior properties over crystalline materials such as higher electrical resistivity, flexibility without loss of hardness, high tensile strength and better corrosion resistance. The iron-based alloys ribbons such as $Fe_{81}B_{13.5}Si_{3.5}C_2$ and $Fe_{67}Co_{18}Si_1B_{14}$ combine high saturation induction, very high permeability and relatively high magnetostriction with low loss hysteresis [5]. Magnetic properties of the evaporated iron-based amorphous thin films were widely investigated for magnetoelastic sensor applications [6,7]. Using RC system $Fe_{81}Co_{13.5}Si_{3.5}C_2$ and $Fe_{67}Co_{18}Si_1B_{14}$ amorphous films evaporated on plastic kapton substrate exhibits a coercivity variation of 2.3 kA/m and/or higher in our previous study [8]. The coercivities of these films are very high as compared to those of the equivalent bulk materials; in some cases are over 2000 larger than their ribbon counterparts. Other researches [9] have also indicated very high coercivities for sputtered and laser-deposited $Fe_{67}Co_{18}Si_1B_{14}$ amorphous films.

The aim of this work was to investigate the feasibility of producing low coercivity $Fe_{81}Co_{13.5}Si_{3.5}C_2$ and $Fe_{67}Co_{18}Si_1B_{14}$ amorphous films using a novel RC system. 100 nm thick films were produced from a resistively heated furnace. Orthogonal design process was applied in order to systematically evaluate the deposition process and parameters, and their corresponding output functions. The correlations between deposition parameters and the output functions have been discussed and presented in this paper.

2 Experimental details

Amorphous ribbons of atomic composition $Fe_{81}Co_{13.5}Si_{3.5}C_2$ and $Fe_{67}Co_{18}Si_1B_{14}$ were used as source material. The thin films were deposited on to a polyimide (Kapton^{TM}) substrate. The substrate was attached to the drum of the RC at ambient temperature, which was later filled with liquid nitrogen and rotated at 1300 rpm. The RC system was operated for an hour for each experiment. The structural analysis of the films was done using a Philips PW1820 X-ray diffractometer. A purpose built Magneto-Optic Loop Plotter (MOKE), operating in transverse Kerr mode, is used to measure the coercivity of the films.

[a] e-mail: hkockar@balikesir.edu.tr

The orthogonal design [10] is based on studying the relationship between input parameters and their corresponding output functions by selecting certain representative combinations of the input parameter level settings. These level settings fit into certain orthogonal tables [11]. The method can be used for process optimisation without having to perform the large number of experiments required by the full factorial design. The simplest method of process optimisation is the one-dimensional research. The other extreme is a full dimensional research exemplified by factorial designs. A number of fractional factorial design approaches have been developed in which certain subsets of the full dimensional search are used to optimise the process. One such approach is orthogonal design, which was developed by Taguchi [12]. The maximum amount of information can be gained by following orthogonal tables. In this case, 4 factors (furnace shape, mass of materials, furnace power and gap between source and the substrate) with 3 levels requires only 9 experimental runs, instead of 81 runs needed to achieve the optimised conditions in the full dimensional space. The theory and application of orthogonal design technique are outside of the scope of this paper and can be found in detailed elsewhere [10–12]. It has a broad application areas such as; optimisation of thin film deposition equipment, plasma etching, photoresist processing, and optical stepper development.

3 Results and discussion

In the RC system, it is possible to vary the furnace shape, the mass of material, the power of furnace, and the gap between substrate and source. Thus, these four variables serve as our input parameters. Starting with a baseline process using (2 mm wide × 4 mm long) furnace shape, 90 mg of material, 355 Watt furnace power, and 24 mm gap between the furnace and the substrate, a level variation using one higher and one lower level was selected, yielding 3 level settings for each input parameter. The input parameters and level settings chosen are summarised in Table 1. The output functions of interest in this work are the coercivity of $Fe_{81}Co_{13.5}Si_{3.5}C_2$ film, denoted as H (A/m), and the coercivity of $Fe_{67}Co_{18}Si_1B_{14}$ film, denoted as H (A/m), respectively. In the experimental setup, four input parameters, each of them with three level settings, fit the orthogonal matrix $L_9 3^4$ [13,14]. In Table 2, the results for each of the 9 experiments required by the $L_9 3^4$ matrix are listed, plus two extra experiments labelled $1'$ and $1''$. These experiments are the repeats of the first experiment and give a useful gauge of the random variation in the process.

Looking at the experiment listed in Table 2, run 1, the conditions chosen were level setting 1 for each of the input parameters, (4×4) mm^2 furnace shape, 60 mg iron, 330 Watt furnace power, and 20 mm gap. These conditions resulted in a coercivity of 136 A/m for $Fe_{81}Co_{13.5}Si_{3.5}C_2$ amorphous film and of 220 A/m for $Fe_{67}Co_{18}Si_1B_{14}$ amorphous film in Table 2. Similarly, the data for each of the other experimental conditions in Table 2 and the corresponding results in Table 4 are listed.

Table 1. The input parameters and level settings used for evaporating thin iron films. Furnace shape is denoted as [width × length] mm^2.

	Input Parameters			
Level Setting 3	Furnace Shape (mm^2)	Mass of Material (mg)	Furnace Power (Watt)	Gap (mm)
1	4×4	060	330	20
2	2×4	090	355	24
3	4×2	120	380	28

The first order data analysis, which is sufficient in the vast majority of process optimisation and characterisation work, proceeds as follows: The output function average (arithmetic means) for each level setting and for each input parameter are determined and listed in Table 4. Thus the coercivity average of $Fe_{81}Co_{13.5}Si_{3.5}C_2$ film for furnace shape setting 1 of (4×4) mm^2 (runs 1, 2, and 3) is given by the average of H_1(213 A/m), H_2(589 A/m), and H_3(193 A/m). This is denoted as Hs_1 and is 348 A/m. The average of the same three runs [H_1(136 A/m), $H_{1'}$(268 A/m), $H_{1''}$(236 A/m)] is taken as H_1 (213 A/m) for run 1. Similarly, the coercivity average of $Fe_{81}Co_{13.5}Si_{3.5}C_2$ film for furnace shape setting 2, (2×4) mm^2, is given by the average of the coercivity for experiments 4, 5 and 6 and is $Hs_2 = 287$ A/m. The coercivity average of $Fe_{81}Co_{13.5}Si_{3.5}C_2$ film for furnace shape setting 3 is $Hs_3 = 229$ A/m. The formulae used in calculating the output function averages are given in Table 3. As can be seen in Table 4, the first order effect of changing the furnace shape (4×4) mm^2, (2×4) mm^2, and (4×2) mm^2 is to decrease the coercivity of $Fe_{81}Co_{13.5}Si_{3.5}C_2$ film from 348 A/m, 287 A/m and finally to 229 A/m, respectively.

Continuing in the same vein, the output functions averages for each of the input parameter levels can be calculated for the coercivity of $Fe_{81}Co_{13.5}Si_{3.5}C_2$ and $Fe_{67}Co_{18}Si_1B_{14}$ amorphous films. This was done and shown in Table 4. The simplified approach to quantify the effect of each input parameter on the output function is to calculate the difference between the maximum and minimum values for each set of output function averages (ΔH, ΔC). The coercivity difference of $Fe_{81}Co_{13.5}Si_{3.5}C_2$ film for furnace shape, ΔHs, is $Hs_1 - Hs_3$, or 118 A/m. Similarly the coercivity difference of $Fe_{81}Co_{13.5}Si_{3.5}C_2$ film for mass is given by $\Delta Hm = Hm_1 - Hm_3$ or 201 A/m. In our case, it can be seen that the smallest coercivity difference for $Fe_{81}Co_{13.5}Si_{3.5}C_2$ film (ΔHg) is 101 A/m that is due to the gap between the substrate and furnace. These output function differences formulae are shown in Table 3. The calculated values of the output function differences are shown in Table 4. By comparing the four differences, it is possible to quantify the relative effect of each input parameter on the coercivity of $Fe_{81}Co_{13.5}Si_{3.5}C_2$ film over the level setting range chosen for that parameter. It should be emphasised that this approach to data analysis is the simplest approach; more sophisticated statistical approaches can be found elsewhere [14,15].

Table 2. The orthogonal experimental results for coercivity of films (A/m).

	Input Parameters				Output Functions	
Run	F. Shape (mm^2)	Mass (mg)	Power (Watt)	Gap (mm)	Coercivity of $Fe_{81}Co_{13.5}Si_{3.5}C_2$ H, (A/m)	Coercivity of $Fe_{67}Co_{18}Si_1B_{14}$ C, (A/m)
1	(1) 4×4	(1) 060	(1) 330	(1) 20	$H_1 = 136$	$C_1 = 220$
2	(1) 4×4	(2) 090	(2) 355	(2) 24	$H_2 = 589$	$C_2 = 1031$
3	(1) 4×4	(3) 120	(3) 380	(3) 28	$H_3 = 193$	$C_3 = 330$
4	(2) 2×4	(1) 060	(2) 355	(3) 28	$H_4 = 425$	$C_4 = 750$
5	(2) 2×4	(2) 090	(3) 380	(1) 20	$H_5 = 168$	$C_5 = 320$
$1'$	(1) 4×4	(1) 060	(1) 330	(1) 20	$H_{1'} = 268$	$C_{1'} = 550$
6	(2) 2×4	(3) 120	(1) 330	(2) 24	$H_6 = 504$	$C_6 = 745$
7	(3) 4×2	(1) 060	(3) 380	(2) 24	$H_7 = 59$	$C_7 = 75$
8	(3) 4×2	(2) 090	(1) 330	(3) 28	$H_8 = 125$	$C_8 = 300$
9	(3) 4×2	(3) 120	(2) 355	(1) 20	$H_9 = 411$	$C_9 = 652$
$1''$	(1) 4×4	(1) 060	(1) 330	(1) 20	$H_{1''} = 236$	$C_{1''} = 413$

Table 3. Formulae for Output Function Averages and Output Function Differences for the Orthogonal Table $L_9 3^4$. (The subscripts used are; s for furnace shape, m for mass, p for furnace power, g for gap between the substrate and resistively heated furnace.)

$Hs_1 = {}^1/_3(H_1 + H_2 + H_3)$	$Hm_1 = {}^1/_3(H_1 + H_4 + H_7)$
$Hs_2 = {}^1/_3(H_4 + H_5 + H_6)$	$Hm_2 = {}^1/_3(H_2 + H_5 + H_8)$
$Hs_3 = {}^1/_3(H_7 + H_8 + H_9)$	$Hm_3 = {}^1/_3(H_3 + H_6 + H_9)$
$\Delta Hs = Hs(\text{max.}) - Hs(\text{min.})$	$\Delta Hm = Hm(\text{max.}) - Hm(\text{min.})$
$Hp_1 = {}^1/_3(H_1 + H_6 + H_8)$	$Hg_1 = {}^1/_3(H_1 + H_5 + H_9)$
$Hp_2 = {}^1/_3(H_2 + H_4 + H_9)$	$Hg_2 = {}^1/_3(H_2 + H_6 + H_7)$
$Hp_3 = {}^1/_3(H_3 + H_5 + H_7)$	$Hg_3 = {}^1/_3(H_3 + H_4 + H_8)$
$\Delta Hp = Hp(\text{max.}) - Hp(\text{min.})$	$\Delta Hg = Hg(\text{max.}) - Hg(\text{min.})$

Table 4. The corresponding analysis of Table 3 for Output Function Averages and Output Function Differences, and Standard Deviations.

	Analysis of the results				
Run	F. Shape (mm^2)	Mass (mg)	Power (Watt)	Gap (mm)	Standard déviations
H_1	$Hs_1 = 348$	$Hm_1 = 396$	$Hp_1 = 196$	$Hg_1 = 56$	
H_2	$Hs_2 = 287$	$Hm_2 = 272$	$Hp_2 = 380$	$Hg_2 = 157$	
H_3	$Hs_3 = 229$	$Hm_3 = 195$	$Hp_3 = 288$	$Hg_3 = 120$	
ΔH	$\Delta Hs = 118$	$\Delta Hm = 201$	$\Delta Hp = 184$	$\Delta Hg = 101$	Std $Dev_H = 49$
C_1	$Cs_1 = 596$	$Cm_1 = 641$	$Cp_1 = 351$	$Cg_1 = 83$	
C_2	$Cs_2 = 540$	$Cm_2 = 475$	$Cp_2 = 694$	$Cg_2 = 242$	
C_3	$Cs_3 = 373$	$Cm_3 = 393$	$Cp_3 = 465$	$Cg_3 = 238$	
ΔC	$\Delta Cs = 223$	$\Delta Cm = 248$	$\Delta Cp = 343$	$\Delta Cg = 160$	Std $Dev_C = 76$

It is now easy to determine a process that will yield the lowest coercivity of $Fe_{81}Co_{13.5}Si_{3.5}C_2$ film. Table 4 shows that lowest coercivity of $Fe_{81}Co_{13.5}Si_{3.5}C_2$ film for each input parameter occurs at the (4×2) mm^2 furnace shape, the largest amount of material, the lowest power and a smallest gap of 20 mm. The process is optimised at these level settings with the goal of attaining an $Fe_{81}Co_{13.5}Si_{3.5}C_2$ film with low coercivity. This recipe, represented by level settings 3, 3, 1, 1 for furnace shape, mass, power, and gap respectively, is not one of the experiments included in the original $L_9 3^4$ orthogonal matrix. Going back to the RC system and running this recipe is expected to give a lower coercivity value than any of the coercivity values obtained in the 9 original experiments. By comparing the output function differences (ΔHs, ΔHm, ΔHp and ΔHg) with standard deviation for coercivity, the output function differences for all input parameters is higher than the standard deviation of the coercivity values for $Fe_{81}Co_{13.5}Si_{3.5}C_2$ films, which means all input parameters have a variation effect on coercivity values.

Moreover, the redundant experimental runs, 1, $1'$ and $1''$, can be used to compute the random variation

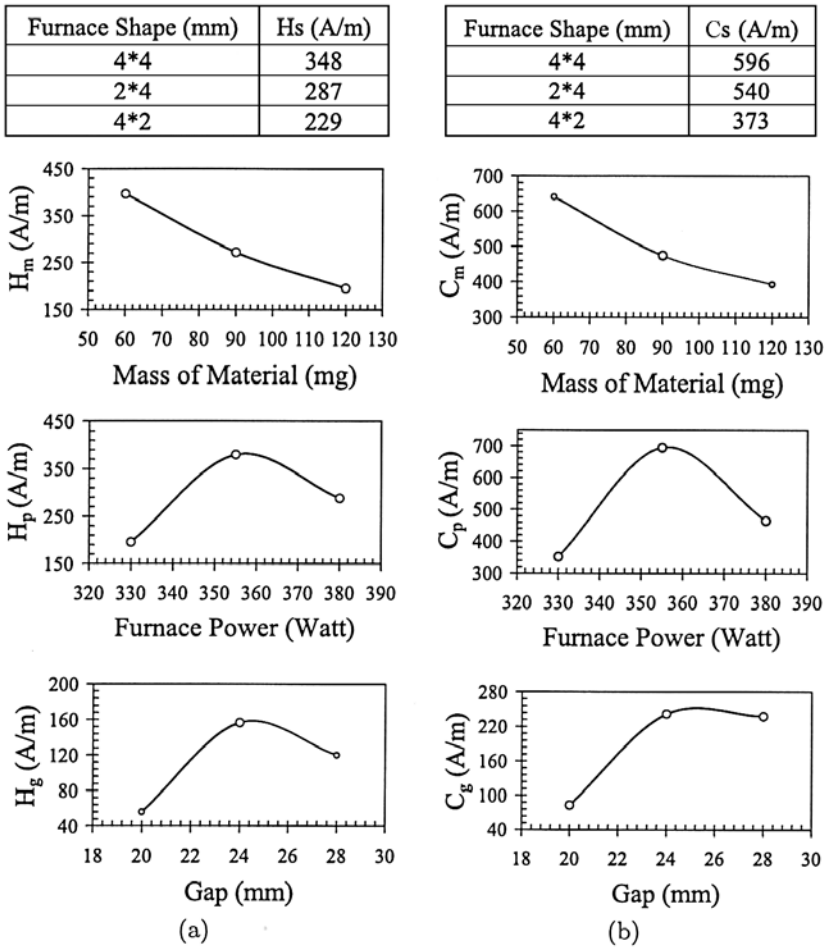

Fig. 1. A plot of the output function averages from Table 4 as a function of the input parameter level settings, (a) $Fe_{81}Co_{13.5}Si_{3.5}C_2$ film and (b) $Fe_{67}Co_{18}Si_1B_{14}$ film.

in the process. This is done by using the results from 1, 1′ and 1″ to calculate the standard deviation. The relative significance of the output function averages can then be determined by comparison to the standard deviation. Without going into the details of statistical comparison techniques, it can be stated that for experiments of this type, with relatively few repetitions, an output function difference of 2 to 3 standard deviations will be needed before the results begin to be significant.

In this work, the coercivity of $Fe_{81}Co_{13.5}Si_{3.5}C_2$ film has not been the sole subject of the discussion, but coercivity of $Fe_{67}Co_{18}Si_1B_{14}$ film is also important in developing an optimal process. In examining the averages and differences for the coercivity of $Fe_{67}Co_{18}Si_1B_{14}$ film is also shown in Table 4, with the goal of having the lowest coercivity of the films, the following recipe would be chosen, as 3, 3, 1, 1.

The lowest coercivity values for both films are gained at furnace shape level 3, mass of material 3, power of furnace 1 ant the gap between substrate and source 1. Therefore, the optimum output parameters would be; 3, 3, 1, 1. The subsequent coercivity of $Fe_{81}Co_{13.5}Si_{3.5}C_2$ film and $Fe_{67}Co_{18}Si_1B_{14}$ film results derived using this recipe are 12 A/m and 28 nm/s. These results are a substantial improvement over the results seen in the eleven experimental runs required by the orthogonal matrix.

Further information can be gained from the orthogonal matrix by plotting the level averages for $Fe_{81}Co_{13.5}Si_{3.5}C_2$ film and $Fe_{67}Co_{18}Si_1B_{14}$ film as a function of level setting in Figure 1a and Figure 1b, respectively. As it can be seen in Figure 1a and Figure 1b, if the level settings are extended beyond the chosen for original matrix, it should be possible to achieve even lower coercivity for both films. In practice, due to the limitation of the RC system it cannot exceed those values used in the experimental system. Such as in the case of mass of material, the lowest coercivity is obtained at 120 mg, and a greater rate could be achieved by going to a mass of more than 120 mg. However, due to the limitation of volume of the furnace it cannot exceed those values used in the level settings for the mass of the iron powder.

Although the results indicate that the process can be easily optimised; there is more effect of some production parameters by looking at the standard deviation values. Furthermore, the large standard deviations over the optimised measurements are thought to be in part due to the difficulty in maintaining consistent deposition parameters.

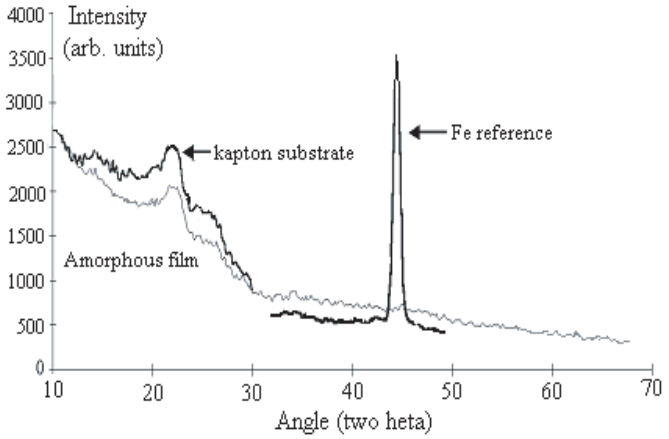

Fig. 2. X-ray diffraction pattern for an amorphous film deposited using $Fe_{81}Co_{13.5}Si_{3.5}C_2$ ribbon as the source material.

Figure 2 shows the X-ray diffraction trace for a film deposited on Kapton using $Fe_{81}Co_{13.5}Si_{3.5}C_2$ ribbon as the source material. To check the validity of the measurement, a reference film also measured along with an uncoated Kapton substrate. The iron reference gives a strong Bragg diffraction peak, confirming the presence of a polycrystalline α-Fe phase. The amorphous film produces an almost identical trace to hat of blank Kapton substrate indicating the absence of a crystalline phase and hence, an amorphous structure. Compositional analysis obtained using Inductively Coupled Plasma Atomic Emission Spectrometry (ICP-AS) and Scanning Electron Microscopy (SEM) indicated only small variations of film composition from the original amorphous ribbon source material.

4 Conclusion

The orthogonal process technique was applied for the purpose of producing low coercivity amorphous thin films for the sensor application. The optimum low coercivity films production process was obtained, by using the chosen control parameters. The results of orthogonal analysis indicate that there is an effect of all input on coercivity, depending on the standard deviation values. The large standard deviations over the optimised measurements are thought to be in part due to the difficulty in maintaining consistent deposition condition.

The author would like to thank Balikesir University, Turkey for the support for this study. Thanks also go to Wolfson Centre, Cardiff University, UK for providing facilities during the major part of the experimental work. Balikesir University, Research Centre of Applied Sciences (BURCAS), Turkey is greatly acknowledged for ICP-AES analysis of films.

References

1. H. Kockar, T. Meydan, Eur. Phys. J. A **17**, 209 (2002)
2. H. Kockar, T. Meydan, J. Magn. Magn. Mater. **242**, 183 (2002)
3. H. Kockar, T. Meydan, J. Magn. Magn. Mater. **242**, 187 (2002)
4. H. Kockar, T. Meydan, Physica B **321**, 124 (2002)
5. *Metglass Magnetic Alloys Catalogue* (Allied Signal Inc. USA, 1986)
6. H. Chiriac, M. Pletea, E. Hristoforou, Sensor Actuators A-Phys. **68**, 414 (1998)
7. H. Chiriac, M. Pletea, E. Hristoforou, Sensor Actuators A-Phys. **81**, 166 (2000)
8. H. Kockar, T. Meydan, The European Pysical J. B **26**, 435 (2002)
9. T. Meydan, P.I. Williams, A.N. Grigorenko, P.I. Nikitin, A. Perone, A. Zocco, Sensor Actuators A-Phys. **81**, 254 (2000)
10. W.G. Cochran, G.M. Cox, Experimental Design (John Willey & Sons, NY, 1957)
11. O. Kempthorn, *The Design and Analysis of Experiments* (R.E. Krieger Publishing Co., Huntington, NY, 1979)
12. G. Taguchi, *Experimental Designs*, 3rd edn., Vol. 2 (Maruzen Publishing Co., Tokyo, Japan, 1977)
13. R.N. Kackar, J. Quality Technology **17**, 176 (1985)
14. D. Raghavarao, *Construction and Combinatorial Problems in Design of Experiments* (John Willey & Sons, NY, 1971)
15. W.J. Diamond, *Practical Experiment Designs* (Van Nostrand Reinhold Co., NY, 1981)